

Use of EIS, Polarization and Electrochemical Noise Measurements to Monitor the Copper Corrosion in chloride media at different temperatures

Weiwei Cheng¹, Shengyun Luo², Yu Chen^{2,3,*}

¹ School of Information Science and Technology, Zhejiang Sci-Tech University, Hangzhou, Zhejiang 310018, China

² School of Materials Science and Engineering, Guizhou Minzu University, Guizhou, Guiyang 550025, China

³ Department of Chemical Engineering and Safety, Binzhou University, Binzhou, Shandong 256600, China

*E-mail: chen123yu123@163.com

Received: 8 January 2019/ Accepted: 28 February 2019 / Published: 10 April 2019

Different electrochemical methods were applied to monitor the copper corrosion behavior in 0.06 mol/L NaCl solution. Some important electrochemical parameters, including the polarization resistance R_p and charge transfer resistance R_{ct} were derived from linear polarization and electrochemical impedance spectroscopy, respectively. The results indicated that the calculated noise resistance R_n , which was obtained from moving average removal (MAR) or polynomial trend removal (PTR) trend removal method, could not equate with R_p or R_{ct} in the present study. However, the active pitting energy E_c , deduced from FWT method without trend removal technique, shows the similar variation trend with R_p or R_{ct} . Hence, electrochemical noise can be utilized as a nondestructive technique to on-line monitor the corrosion progress which can be performed with simple equipment. Furthermore, the deduced parameter E_c presents closer relation to the metal surface structure and shows the same variation trend with the corrosion rate and severity.

Keywords: copper; electrochemical noise; trend removal

1. INTRODUCTION

Electrochemical noise (EN) technique is a more efficient and accurate method to monitor the corrosion process comparing with other classical electrochemical methods, such as potentiodynamic polarization, linear polarization and electrochemical impedance spectroscopy (EIS), due to its non-destructive and non-intrusive nature [1-12].

Up to now, several mathematical methods have been explored to analyze the electrochemical noise data in both qualitative and quantitative way. Initially, a simple way to analyze the electrochemical noise data was in the time domain and some useful information can be obtained from the frequency and the shape of potential and current transients, which generally represents the corrosion type and indicates the pit formation [13]. Statistical method has been utilized and some informative parameters were proposed to identify various types of corrosion processes when studying the 304L stainless steel (UNS S30403) corrosion process in 0.05 M ferric chloride (FeCl_3) solution [14]. EN technique has also been used to evaluate the materials susceptibility to stress corrosion cracking (SCC) and it was found that the EN reading had transients with high intensity and frequency when the steel was immune to stress corrosion cracking, while presented transients that decreased toward the final fracture when it was susceptible to stress corrosion cracking. This finding was further certified by Nyquist diagrams [15]. Additionally, electrochemical noise resistance R_n is another important parameter to evaluate corrosion resistance which value was calculated from the ratio of the standard deviation of potential noise to the standard deviation of current noise [16-19]. Several experimental [20,21] and theoretical [22-24] efforts have been made to conclude that R_n is a reliable parameter of corrosion resistance and in most cases equivalent to polarization resistance (R_p) and therefore R_p can be replaced by R_n in Stern Geary equation to calculate the corrosion rate. Allahar [25] has tracked the cathodic protection performance of Mg-rich primer using EN technique and both of the calculated localized index and noise resistance R_n suggested the feasibility of electrochemical noise measurement for in-situ predicting the cathodic protection. Generally, R_n is expected to be in consistent with R_p only for systems showing high corrosion rates for the reason that the impedance spectrum has reached the dc limit within Δf [26]. However, some researches [27,28] acclaim that R_p and R_n are not always equal, and the relation of R_n and corrosion degradation process is under investigation.

Power spectral density (PSD) plots which can be derived from the mathematic procedure of Fast Fourier Transform (FFT) and Maximum Entropy Method (MEM) in the frequency domain is another powerful method. Some useful parameters, including the low frequency plateau W , the critical frequency f_c and the slope of high frequency liner region k can give us insight into the corrosion mechanism [29]. It is generally believed that localized corrosion occurred when the slope k was higher than -20 dB/decade, while a lower value than -20 dB/decade or even smaller than -40 dB/decade represented the uniform corrosion [30].

It is known that all the above mentioned methods to analyze electrochemical noise data are based on the trend removal of the original data. Disappointingly, there was still strong controversy on the validity of different trend removal methods, such as linear trend removal (LTR), polynomial trend removal (PTR) method [31] and moving average removal (MAR) [32]. Some unsatisfactory aspects still exist due to their damage to the original signals [33]. Fast wavelet transformation (FWT) technique is another powerful method to analyze the electrochemical noise data, during which the dc trend is not necessary to be removed and thus eliminate the defects of the FFT and MEM methods [34]. Moreover, different corrosion events with different timescales can be separated from relative energy distribution plot (EDP) obtained from FWT analysis [35]. When studying the electroplating of zinc, the maximum relative energy moved from the region with larger scales to those with smaller

scales and the structure of obtained deposits changed from dendritic to compact [36]. Furthermore, the crystal growth energy showed the same variation trend with crystallite size in case of tin electrodeposition [37]. However, a systematic comparison of these analyzing methods to monitor the metal corrosion or electrodeposition process has been rarely reported.

The corrosion behavior of copper in 0.06 mol/L NaCl solution has been investigated in the previous study [38] which was focused on the effect of sampling frequency on the energy distribution plot and the PSD spectra was discussed. The aim of the present work is to compare the results of different electrochemical methods on monitoring the copper corrosion process, especially evaluate the effect of trend removal methods on the analysis of electrochemical noise data.

2. EXPERIMENTAL

0.06 mol/L NaCl solution was used as corrosive media and prepared from analytical grade NaCl (Sinopharm Chemical Reagent Co., Ltd.) and double distilled water. High purity copper specimens (99.99%) obtained from Sigma-Aldrich company was served as working electrode. The copper electrode was embedded into Teflon and only a surface area of 0.50 cm² was exposed to the corrosive media. Prior to the measurements, the exposed copper surface was polished to mirror mechanically, washed with double distilled water and then dried with cool N₂. Electrochemical experiments were conducted using a traditional three-electrode electrochemical department. A saturated calomel electrode (SCE) and Pt mesh of large area were adopted as reference and auxiliary electrode, respectively.

EIS measurements were performed using a PARSTAT 2273 impedance measurement unit. The scanning frequency was initiated from 100 kHz to 10 mHz. All the EIS measurements were conducted at the open circuit potential (E_{ocp}) and the amplitude of sinusoidal perturbation of 5 mV was applied. Before the measurements, the pre-treated copper electrodes were always immersed into the corrosive media for at least 30 min until the value of E_{ocp} was steady. All the measurements were carried out in a quiescent state and a thermostatically water bath was used to stabilize the experimental temperature. Z-View software was applied to simulate the EIS data to get some useful electrochemical parameters. Each temperature was conducted at least three times in parallel and the average results were reported. Linear polarization measurements were carried out using CHI660A electrochemical workstation at a scanning rate of 1 mV/s and the testing potential range was $E_{ocp}-10$ mV to $E_{ocp}+10$ mV.

Both of the electrochemical current noise and electrochemical potential noise which was generated during the copper corrosion in 0.06 mol/L NaCl solution at E_{ocp} , were recorded using an automatic zero resistance ammeter (ZRA) technique at a sampling rate of 8 Hz [39]. Two identical copper working electrodes were employed and kept in a stable parallel position in the corrosive media. During the measurements, the EN testing device was shielded in a Faradaic cage. The copper surface morphologies after corroded in 0.06 mol/L NaCl solution at different temperatures were recorded with SEM and have been reported in the previous work [38].

3. RESULTS AND DISCUSSION

Fig.1 shows the linear polarization curves for copper corrosion in 0.06 mol/L NaCl solution at different temperatures. The values of polarization resistance were calculated from the slope and the results are summarized in Table 1. Obviously, with increasing the testing temperature from 20°C to 40°C, the R_p values decreased from 4458 $\Omega \cdot \text{cm}^2$ to 1313 $\Omega \cdot \text{cm}^2$, indicating that the raise of temperature accelerated the dissolution process of copper in 0.06 mol/L NaCl solution [40].

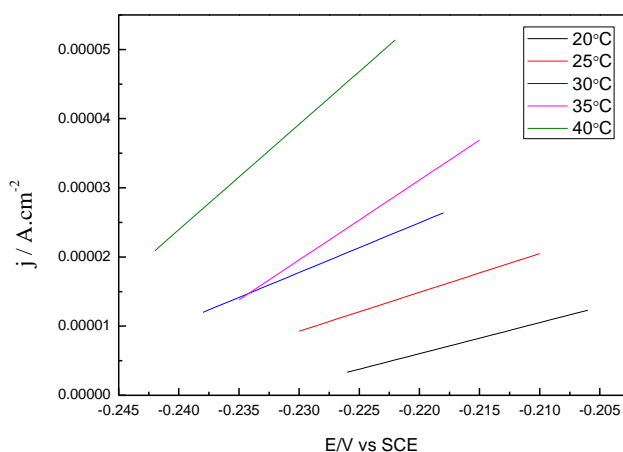


Figure 1. Linear polarization curves for copper corrosion in 0.06 mol/L NaCl solution at different temperatures.

Table 1. Polarization resistance R_p of copper corrosion in 0.06 mol/L NaCl solution.

	20°C	25°C	30°C	35°C	40°C
$R_p(\Omega \cdot \text{cm}^2)$	4458	3560	2780	1731	1313

The Nyquist and Bode plots for copper corrosion in 0.06 mol/L NaCl solution at different temperatures are depicted in Fig.2. It can be seen that the impedance decreases with increasing testing temperature. Under different testing temperatures, the Nyquist plots present two differentiable capacitances and Bode plots always show two phase angle peaks. Moreover, the semi-circles in Nyquist plots are not perfect and the circle centers are observed to be below the real axis, indicating a non-ideal electrochemical behavior at the copper/ liquid interface [41], which may be ascribed to the heterogeneities of copper surface [42]. According to the method developed by Wit [43,44] and the characteristics of both the Bode plots and Nyquist plots (such as the number of the slopes and the number of the phase angle peaks in Bode plot, and the number of the capacitance in Nyquist plot) simultaneously, it can be deduced that the EIS plots consist of two capacitances and a Warburg diffusion element in our experimental condition. This EIS feature has also been reported in the previous reference [45]. The two capacitances located at high and middle frequency may be corresponding to electrochemical process and corrosion products at the interface, respectively. It is also noticeable that the shape of Nyquist and Bode plots did not change with increasing testing temperatures, revealing that the corrosion mechanism is the same at different temperatures [46].

Therefore, the equivalent electrochemical circuit (EEC) as shown in Fig.3 was employed to quantitatively analyze the copper corrosion in 0.06 mol/L NaCl solution and the derived electrochemical parameters were listed in Table 2.

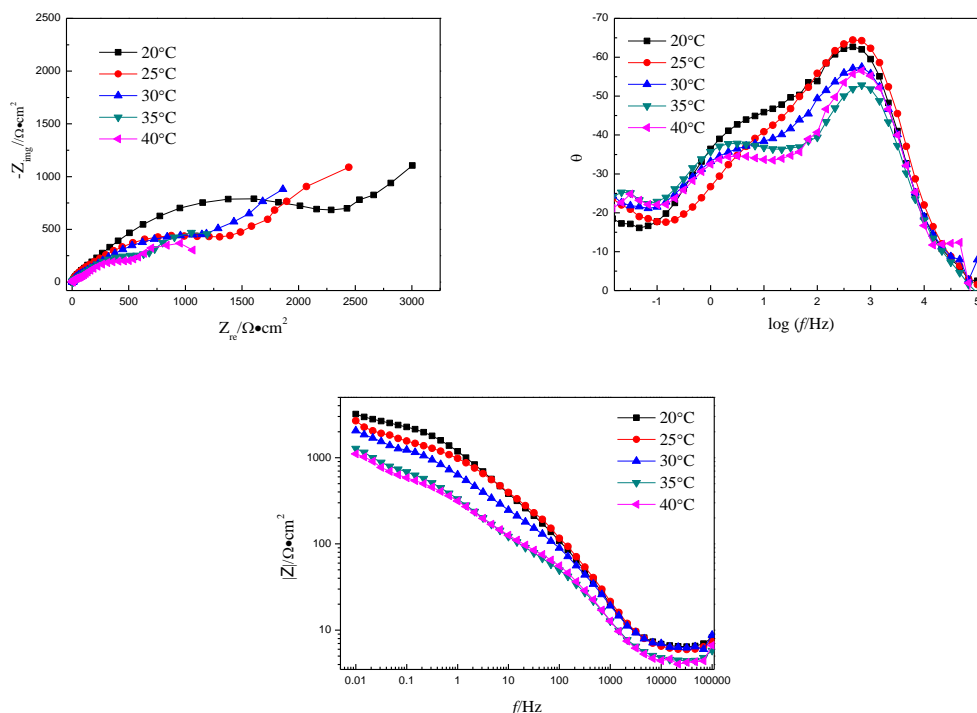


Figure 2. Nyquist and Bode plots for copper corrosion in 0.06 mol/L NaCl solution at different temperatures.

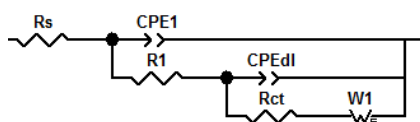


Figure 3. EEC for copper corrosion in 0.06 mol/L NaCl solution at different temperatures. R_s is the solution resistance, CPE_1 and R_1 corresponds to the film capacitance and the film resistance, respectively. CPE_{dl} and R_{ct} represent the double layer capacitance and the charge transfer resistance, respectively. W_1 is the Warburg diffusion element.

Table 2. Impedance parameters of copper corrosion at different temperatures.

	20°C	25°C	30°C	35°C	40°C
$R_s(\Omega \cdot \text{cm}^2)$	4.58	5.26	6.64	4.91	5.83
$CPE_1(\mu\text{F} \cdot \text{cm}^2)$	3.64	2.48	3.78	6.56	4.93
n1	0.942	0.976	0.948	0.929	0.961
$R_1(\Omega \cdot \text{cm}^2)$	142.8	92.5	76.8	47.9	54.1
$CPE_{dl}(\mu\text{F} \cdot \text{cm}^2)$	49.3	62.0	124	216	232
n2	0.615	0.526	0.521	0.594	0.587
$R_{ct}(\Omega \cdot \text{cm}^2)$	2663	1733	1635.5	742.6	544.5
$W(\Omega \cdot \text{cm}^2)$	2869.5	2456.5	2048.5	1381.5	916.5

From **Table 2**, it can be seen that the R_s values range from 4.58 to 6.64 $\Omega \cdot \text{cm}^2$ at different temperatures, suggesting that the ohmic drop between reference electrode and working electrode through the electrolyte has been minimized in this experimental department. In this work, the sum of R_1 , R_{ct} and diffusion impedance (W) is used to represent corrosion resistance due to the involvement of O_2 reduction during copper corrosion process. Generally, the larger the sum value, the slower the corrosion rate. Apparently, with raising temperature, the sum of R_1 , R_{ct} and diffusion impedance (W) decreased from 5675.3 $\Omega \cdot \text{cm}^2$ to 1515.1 $\Omega \cdot \text{cm}^2$, suggesting that the corrosion rate inclined with the increase of temperature. This finding agreed well with the linear polarization studies.

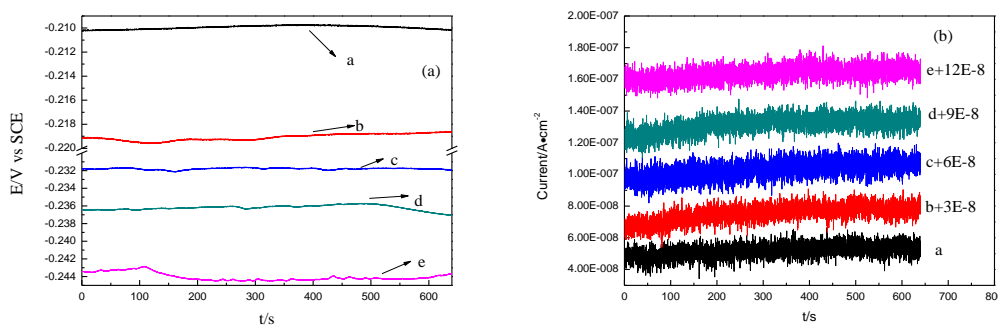


Figure 4. (a) Potential and (b) current noise data at different temperatures: a - 20°C; b - 25°C; c - 30°C; d - 35°C; e - 40°C.

Fig.4 shows the potential and current noise of copper corrosion in 0.06 mol/L NaCl solution at different testing temperatures by ZRA technique. It can be seen that with increasing testing temperature, the corrosion potential moves in the negative direction, whereas the current density did not change much. Arman [47] has studied the corrosion protection performance of an epoxy zinc-rich coating implanted with different particles. They calculated the noise resistance R_n values based on the second order statistics from EN measurements and found that the micaceous iron oxide loaded coating possessed better protection properties. In the present work, both MAR [48] and PTR [31] trend removal methods were used to remove the dc trend, and the deduced noise resistances are recorded as R_{n-MAR} and R_{n-PTR} , respectively.

For MAR analysis, the individual data point in the group V_n , V_i is composed of dc trend and the random noise which can be expressed as a function of time, t .

$$V_i(t) = V_{i,noise}(t) + V_{i,dc}(t) \tag{1}$$

$V_{i,noise}(t)$ represents the real random noise and is used for EN analysis. $V_{i,dc}(t)$ corresponds to the dc trend which should be deleted. In this method, there is a central assumption that an average value of adjacent data points of V_i which can be taken as an estimation of $V_{i,dc}(t)$. In the present work, 15 data points are selected for calculation:

$$\bar{V}_t = [\sum_{i=-7}^{i+7} V_i] / 15 \tag{2}$$

Therefore, the dc trend in the potential-time record can be deleted and the real random fluctuation $V_{i,noise}$ can be calculated using the following equation:

$$V_{i,noise} = V_i - \bar{V}_i \quad (3)$$

for each potential-time record point, and individual average potential can be calculated and so the average potential is changing.

For PTR analysis, the polynomial is of order 5 and then subtracting the computed curves so as to keep the residuals. Fig.5 shows the schematic diagram of MAR and PTR methods applied for potential-time curve (35°C). It is noted that the dc drift in EN is always nonlinear, and there exist obvious difference between these two dc trend lines.

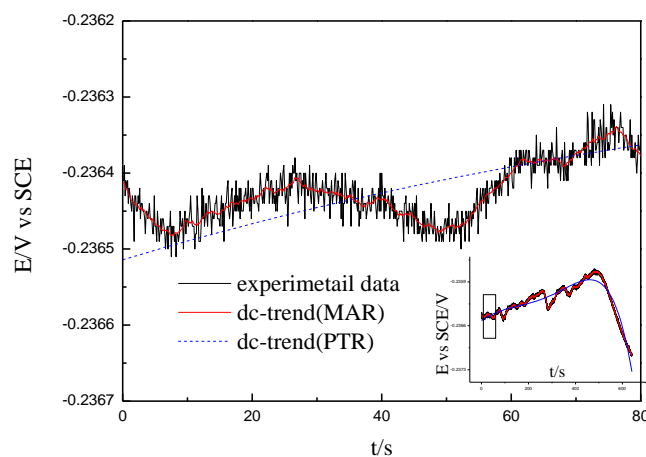


Figure 5. Schematic diagram of MAR and PTR method applied for potential-time curve.

It is clear that, some trend removal methods such as MAR or PTR, may eliminate useful information when removing the dc trend. There exist large deviations between individual and nominally identical measurement. Fig.6 presents the resistance values calculated by different electrochemical methods. It seems that $R_f+R_{ct}+W$, R_p , R_{n-MAR} and R_{n-PTR} decreased with the increasing temperature, however, R_{n-PTR} values are much larger than the others which indicates that the PTR trend removal method is inappropriate for this system. R_{n-MAR} values are comparable to $R_f+R_{ct}+W$ and R_p , although they are not completely equivalent. Even though R_{n-MAR} showed the similar trend with $R_f+R_{ct}+W$ or R_p throughout the whole measuring time, the similarity of R_p and noise resistance is somewhat farfetched. Two possible reasons might explain the scatter: some useful information was removed by MAR technique, or the number of data points to adjust \bar{V}_i is unbecfitting. Hence, the theoretical background and data analysis method still requires further improvement.

In order to qualitatively evaluate the relationship between the EN features and the corrosion severity during copper corrosion in 0.06 M NaCl solution, Fast wavelet transformation (FWT) technique was used to analyze the EN potential data and the obtained energy of different crystals have been reported in the previous study [38]. In addition, the active pitting energy E_c was calculated. It has been reported that the value of E_c showed the same variation trend with corrosion rate when studying the inhibition process and can be utilized to predict the corrosion severity sensitively [49,50]. Moreover, when investigating the adsorption behavior, different variation characteristics of E_c

correspond to different adsorption mechanism, which suggested that E_c was a potential criterion to differentiate the physical and chemical adsorption [51].

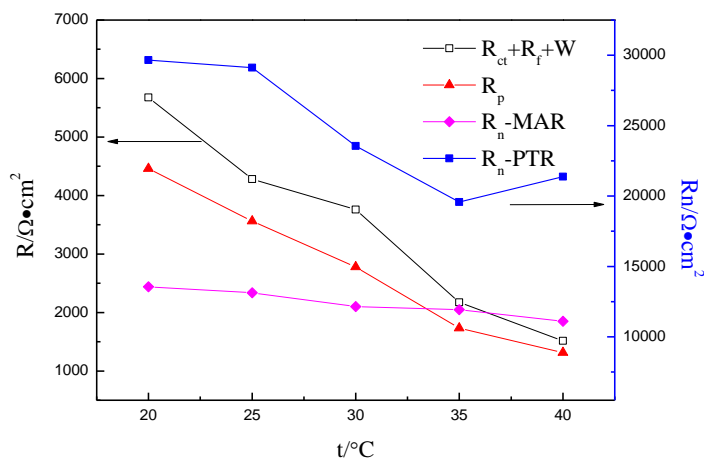


Figure 6. $R_f+R_{ct}+W$, R_p , R_{n-MAR} and R_{n-PTR} for copper in 0.06 M NaCl solution at different temperatures.

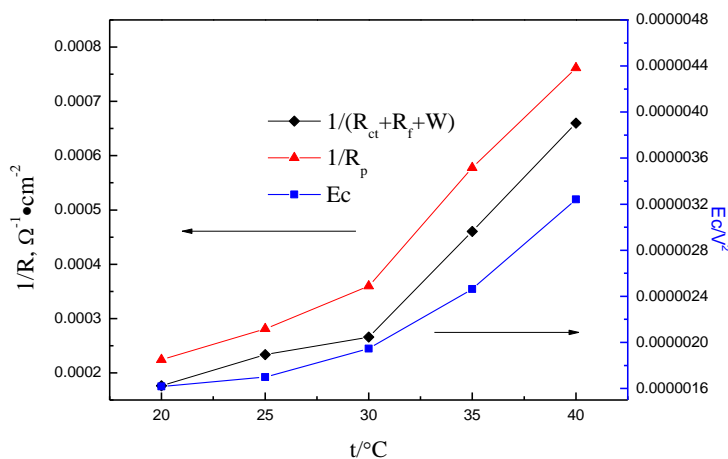


Figure 7. Dependence of E_c on testing temperature, compared with $1/(R_f+R_{ct}+W)$ and $1/R_p$.

The relationship between the E_c with temperature is presented in Fig.7. Apparently, E_c value increases gradually with the increase of temperature, and shows the similar variation trend with the reciprocal of $R_f+R_{ct}+W$ or R_p , which partly represent the corrosion rate. This result also reveals that the active pitting energy obtained from electrochemical noise measurement can not only be used as fingerprint to characteristic the morphology, but also be capable of deducing corrosion rate properly. Comparing to the traditional electrochemical methods, such as polarization resistance and charge transfer resistance calculated from linear polarization and electrochemical impedance spectroscopy, respectively, the electrochemical noise can be utilized as a nondestructive technique to on-line monitor the corrosion progress which can be performed with simple equipment. Furthermore, the deduced

parameter E_c presents closer relation to the metal surface morphology and shows the opposite variation trend with the corrosion rate and severity (SEM results in reference 31).

4. CONCLUSION

The copper corrosion behavior in 0.06 mol/L NaCl solution was studied by linear polarization, electrochemical impedance spectroscopy and electrochemical noise measurements. Results showed that the variation trend of noise resistance R_n with testing temperature, which was calculated through MAR or PTR trend removal method, disagreed with that of polarization resistance R_p and charge transfer resistance R_{ct} , obtained from linear polarization and electrochemical impedance spectroscopy measurements, respectively. However, the active pitting energy E_c , deduced from FWT method without trend removal technique, shows the similar variation trend with R_p or R_{ct} . Hence, electrochemical noise offers a nondestructive and accurate on-line monitoring progress which can be performed with simple equipment. Moreover, the speculated parameter E_c shows closer relation to the surface morphology and corrosion severity.

ACKNOWLEDGEMENT

The authors gratefully acknowledge the financial assistance from the National Natural Science Foundation of China (Project 51771173, 21403194, 51801013) and Zhejiang Provincial Natural Science Foundation of China (LY17F010023).

References

1. Guofu Qiao, Yi Hong and Jinping Ou, *Measurement*, 53 (2014) 270.
2. Z. Sun and F. Mansfeld, *Corrosion*, 55 (1999) 915.
3. X.F. Liu, H.G. Wang and H.C. Gu, *Corros. Sci.*, 48 (2006) 1337.
4. N. Upadhyay, M.G. Pujar, C.R. Das, C. Mallika and U.K. Mudali, *Corrosion*, 70 (2014) 781.
5. Y.Y. Shi, Z. Zhang and J.Q. Zhang, *Electrochim. Acta*, 53 (2008) 2688.
6. G. Suresh and U.K. Mudali, *Corrosion*, 70 (2014) 283.
7. R. Cottis, A. Homborg and J.M.C. Mol, *Electrochim. Acta*, 202 (2016) 277.
8. M. Kiwilszo and J. Smulko, *J. Solid State Electrochem.*, 13 (2008) 1681.
9. M. Shahidi, A.H. Jafari and S.M.A. Hosseini, *Corrosion*, 68 (2012) 1003.
10. J.M. Sanchez-Amaya, R.M. Osuna, M. Bethencourt and F.J. Botana, *Prog. Org. Coat.*, 60 (2007) 248.
11. G.P. Bierwagen, C.S. Jeffcoate, J. Li, S. Balbyshev, D.E. Tallman and D.J. Mills, *Prog. Org. Coat.*, 29 (1996) 21.
12. N. Upadhyay, M.G. Pujar, S.S. Singh, N.G. Krishna, C. Mallika and U.K. Mudali, *Corrosion*, 73 (2017) 1320.
13. D.J. Mills, S.J. Mabbutt and G.P. Bierwagen, *Prog. Org. Coat.*, 46 (2003) 176.
14. G. Suresh and U.K. Mudali, *Corrosion*, 70 (2014) 283.
15. E.J. Carpintero-Moreno, J.G. Gonzalez-Rodriguez, J. Uruchurtu-Chavarin, I. Rosales, B. Campillo and L. Leduc-Lezama, *Corrosion*, 69 (2013) 85.
16. S. Girija, U.K. Mudali and H.S. Khatak, *Corros. Sci.*, 49 (2007) 4051.

17. H. Ashassi-Sorkhabi, D. Seifzadeh and M. Raghbi-Boroujeni, *Arab. J. Chem.*, 9 (2016) S1320.
18. A.M. Homborg, R.A. Cottis and J.M.C. Mol, *Electrochim. Acta*, 222 (2016) 627.
19. S.S. Jamali, D.J. Mills and J.M. Sykes, *Prog. Org. Coat.*, 77 (2014) 733.
20. B. Ramezanzadeh, S.Y. Arman, M. Mehdipour and B.P. Markhali, *Appl. Surf. Sci.*, 289 (2014) 129.
21. U. Bertocci, C. Gabrielli and F. Huet, *J. Electrochem. Soc.*, 144 (1997) 37.
22. U. Bertocci, C. Gabrielli and F. Huet, *J. Electrochem. Soc.*, 144 (1997) 31.
23. J.F. Chen and W.F. Bogaerts, *Corros. Sci.*, 37 (1995) 1839.
24. M. Curioni, R.A. Cottis and G.E. Thompson, *Corrosion*, 69 (2013) 158.
25. K.N. Allahar, Q. Su and G.P. Bierwagen, *Corrosion*, 66 (2012) 1.
26. F. Mansfeld, Z. Sun and C.H. Hsu, *Electrochim. Acta*, 46 (2001) 3651.
27. H. Xiao and F. Mansfeld, *J. Electrochem. Soc.*, 141 (1994) 2332.
28. G. Gusmano, G. Montesperelli and S. Pacetti, *Corrosion*, 53 (1997) 860.
29. F. Mansfeld and H. Xiao, *J. Electrochem. Soc.*, 140 (1993) 2205.
30. C. Gabrielli and M. Keddam, *Corrosion*, 48 (1992) 794.
31. U. Bertocci, F. Huet and R.P. Nogueira, *Corrosion*, 58 (2002) 337.
32. B.P. Markhali, R. Naderi, M. Mahdavian, M. Sayebani and S.Y. Arman, *Corros. Sci.*, 75 (2013) 269.
33. T. Schauer, H. Greisiger and L. Dulog, *Electrochim. Acta*, 43 (1998) 2423.
34. J.J. Kim, *Mater. Lett.*, 61 (2007) 4000.
35. S.M. Hoseinie, A.M. Homborg, T. Shahrabi, J.M.C. Mol and B. Ramezanzadeh, *Electrochim. Acta*, 217 (2016) 226.
36. Z. Zhang, W.H. Leng, Q.Y. Cai, F.H. Cao and J.Q. Zhang, *J. Electrochem. Soc.*, 578 (2005) 357.
37. X.Q. Huang, Y. Chen, T.W. Fu, Z. Zhang and J.Q. Zhang, *J. Electrochem. Soc.*, 160 (2013) D530.
38. Chenxi Yi, Xiaoqing Du, Yumeng Yang, Benfeng Zhu and Zhao Zhang, *RSC advances*, 8 (2018) 19208.
39. M. Iannuzzi, C. Mendez, L. Avila-Gray, G. Maio and H. Rincón, *Corrosion*, 66 (2010) 1.
40. H.R. Zhao, Y.L. Xu, C.K. Chen, Y. Chen, Y.W. Liu and Z.N. Yang, *Corrosion*, 74 (2018) 613.
41. M. Hosseini, S.F.L. Mertens, M. Ghorbani and M.R. Arshadi, *Mater. Chem. Phys.*, 78 (2003) 800.
42. R. Solmaz, G. Kardas, M. Culha, B. Yazici and M. Erbil, *Electrochim. Acta*, 53 (2008) 5941.
43. D.H. van der Weijde, E.P.M. van Westing and J.H.W. de Wit, *Corros. Sci.*, 36 (1994) 643.
44. P. Campestrini, E.P.M. van Westing and J.H.W. de Wit, *Electrochim. Acta*, 46 (2001) 2631.
45. Y. Chen, Y.Y. Jiang, Z. Y. Ye and Z. Zhang, *Corrosion*, 69 (2013) 886.
46. Xianghong Li, Xiaoguang Xie, Shuduan Deng and Guanben Du, *Corros. Sci.*, 92 (2015) 136.
47. S.Y. Arman, B. Ramezanzadeh, S. Farghadani, M. Mehdipour and A. Rajabi, *Corros. Sci.*, 77 (2013) 118.
48. Y.J. Tan, S. Bailey and B. Kinsella, *Corros. Sci.*, 38 (1996) 1681.
49. Y.W. Liu, Y. Chen, X.H. Chen, Z.N. Yang, Y. Xie and Z. Zhang, *J. Alloy. Compd.*, 758 (2018) 184.
50. Y. Chen, X.H. Chen, Z.N. Yang, Y.W. Liu, H.H. Zhang, J.Y. Yin and Z. Zhang, *J. Taiwan Inst. Chem. E.*, 80 (2017) 908.
51. Y. Chen, X.H. Chen, Y.W. Liu, H.H. Zhang, Y. Xie, Z.N. Yang and Z. Zhang, *J. Chem. Thermodyn.*, 126 (2018) 147.